Molecular Cell, Vol. 7, 1293–1306, June, 2001, Copyright ©2001 by Cell Press

Coupling Met to Specific Pathways Results in Distinct Developmental Outcomes

Flavio Maina,[1,4,5] Guido Panté,[1,2,6] Françoise Helmbacher,[1] Rosa Andres,[3] Annika Porthin,[1,6] Alun M. Davies,[3] Carola Ponzetto,[2] and Rüdiger Klein[1,4,6]

[1] European Molecular Biology Laboratory
Meyerhofstrasse 1
69117 Heidelberg
Germany

[2] Department of Anatomy, Pharmacology, and Forensic Medicine
University of Torino
10126 Torino
Italy

[3] Department of Preclinical Veterinary Sciences
Royal (Dick) School of Veterinary Studies
Edinburgh EH9 1QH
Scotland

Summary

Receptor tyrosine kinases (RTKs) mediate distinct biological responses by stimulating similar intracellular signaling pathways. Whether the specificity of the response is determined by qualitative or quantitative differences in signaling output is not known. We addressed this question in vivo by replacing the multifunctional docking sites of Met, the receptor for hepatocyte growth factor, with specific binding motifs for phosphatidylinositol-3 kinase, Src tyrosine kinase, or Grb2 (Met^{2P}, Met^{2S}, and Met^{2G}, respectively). All three mutants retained normal signaling through the multiadaptor Gab1, but differentially recruited specific effectors. While Met^{2G} mice developed normally, Met^{2P} and Met^{2S} mice were loss-of-function mutants displaying different phenotypes and rescue of distinct tissues. These data indicate that RTK-mediated activation of specific signaling pathways is required to fulfill cell-specific functions in vivo.

Introduction

Upon ligand binding, RTKs dimerize and autophosphorylate on tyrosine (Schlessinger, 2000). Some of the phosphotyrosines are recognized as specific docking sites by intracellular effectors (Pawson and Nash, 2000). Different molecules are recruited depending on the flanking amino acids and on the type of phosphotyrosine binding module carried by the effector. This recruitment/activation triggers several major signaling cascades that elicit the biological response. It is unclear whether distinct biological effects result from the activation of specific pathways or from quantitative differences in generic signaling output (Simon, 2000). A recent study done with PDGF receptor mutants capable of binding only individual effectors has shown qualitatively similar transcriptional outputs (Fambrough et al., 1999), suggesting cross talk among pathways distal to the receptor. However, these results were obtained stimulating transfected cells with saturating concentrations of ligand, a far from normal situation.

The best model for testing the effects of preferential inactivation/activation of individual pathways would be the whole organism. Many RTKs are essential in development; by gene modification, specific Tyr → Phe loss-of-function or add-back mutations can be introduced into the genome and their effects evaluated. By applying this approach to the mouse, we have shown the importance of docking sites for receptor function. The C-terminal portion of Met, the hepatocyte growth factor (HGF) receptor, contains two tandem tyrosines in a degenerate motif, which when phosphorylated, bind different SH2-containing molecules including phosphatidylinositol-3 kinase (PI3K), Src, the Grb2 and Shc adaptors, and the multiadaptor Gab1 (Ponzetto et al., 1994; Fixman et al., 1997; Schaeper et al., 2000, and references within). Mutation of these tyrosines in c-*met* (*met^d*) led to an embryonic lethal phenotype resembling that of a *met* null mutant, with placental, liver, muscle, and nerve defects (Maina et al., 1996, 1997, 1998; reviewed in Birchmeier and Gherardi, 1998). In the present study, we converted these multifunctional docking sites into optimal binding motifs for PI3K, Src, or Grb2 (*met^{2P}*, *met^{2S}*, and *met^{2G}*, specificity-switch mutants), to address in vivo the role of specific pathways in receptor signaling.

To evaluate the signaling potential of the new mutants relative to the severe loss-of-function model (*met^d*), we first assessed the residual ability of Met^d to signal via Gab1. We show that, upon HGF stimulation, Met^d no longer binds but can still transphosphorylate Gab1, although to a lesser extent. Conversely, all the new mutants retain normal Gab1 signaling but also activate specific effectors, resulting in distinct developmental outcomes. This difference in biological read-out supports the idea that in vivo activation of specific intracellular signaling pathways by RTKs is required to achieve the full spectrum of biological responses.

Results

Mutation of Tyrosines in the Met Multifunctional Docking Site (Met^d) Abrogates Gab1 Binding But Only Reduces Gab1 Phosphorylation

We previously knocked in Tyr-Phe mutations in the *met* locus ($Y_{1349}VHVNATY_{1356}VNV \rightarrow F_{1349}VHVNATF_{1356}VNV$, *$met^d$* allele; Figure 1A; Maina et al., 1996). Mice with a wild-type knockin *met* cDNA (*$met^{WT/WT}$*) were normal, while *$met^{d/d}$* mice had a lethal phenotype. Thus, Y_{1349} and Y_{1356} are essential for Met-mediated development. Later, it was shown that the adaptor Gab1 binds to these tyrosines, is phosphorylated, and acts as a signaling ampli-

[4] Correspondence: maina@ibdm.univ-mrs.fr (F.M.), rklein@neuro.mpg.de (R.K.)

[5] Present address: Inserm U382, IBDM, Campus de Luminy-Case 907, Marseille Cedex 09, France.

[6] Present address: Max-Planck Institute of Neurobiology, Am Klopferspitz 18A, D-82152 Martinsried, Germany.

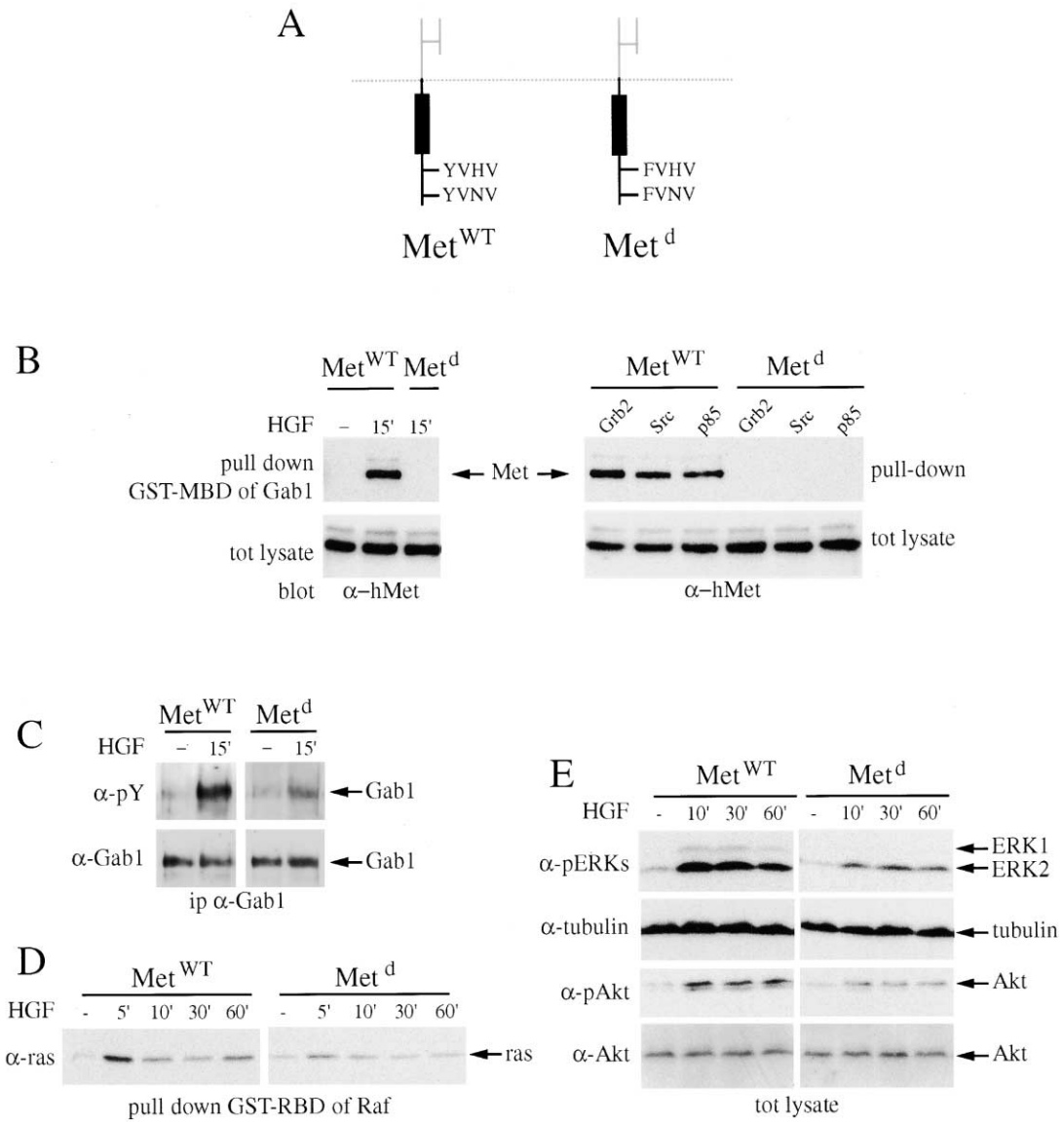

Figure 1. Met^{d} Is Not Signaling Dead

(A) Met receptors previously obtained by the knockin of a human cDNA (wild-type or mutated) into the *met* locus (Maina et al., 1996). Met^{WT}: wild-type chimeric protein (extracellular, mouse, gray; transmembrane and intracellular, human: black) with multifunctional docking sites; Met^{d}: Tyr → Phe mutated chimeric protein, without docking sites.

(B) In vitro binding of Gab1, Grb2, Src, and p85PI3K by Met^{WT} and Met^{d}. GST-fusion proteins of the Gab1 Met binding domain (MBD), the carboxyl-terminal p85PI3K SH2, the Src SH2, and full size Grb2 were immobilized on glutathione-Sepharose and incubated with lysates of untreated or HGF-stimulated *met*$^{WT/WT}$ and *met*$^{d/d}$ hepatocytes. Blots of complexes were probed with anti-human Met antibodies (α-hMet). The amount of Met in each lysate is shown.

(C) HGF-induced Gab1 phosphorylation by Met^{WT} and Met^{d}. Gab1 was immunoprecipitated (IP) from lysates of untreated or HGF-stimulated *met*$^{WT/WT}$ and *met*$^{d/d}$ hepatocytes. IPs were blotted and probed with anti-phosphotyrosine (α-pY) and anti-Gab1 (α-Gab1) antibodies.

(D) Time course of HGF-induced Ras activation by Met^{WT} and Met^{d}. A GST-fusion protein of the Ras binding domain of Raf (RBD) was immobilized on glutathione-Sepharose and incubated with lysates of untreated or HGF-stimulated *met*$^{WT/WT}$ and *met*$^{d/d}$ hepatocytes. The complexes were blotted and probed with anti-Ras antibodies (α-Ras).

(E) Time course of HGF-induced ERK and Akt phosphorylation by Met^{WT} and Met^{d}. Total lysates of *met*$^{WT/WT}$ and *met*$^{d/d}$ hepatocytes, either untreated or HGF-stimulated, were blotted and probed with anti-phospho ERKs (α-pERKs) or Akt (α-pAkt) antibodies and with antibodies against α-tubulin and Akt (α-Akt).

fier (Schaeper et al., 2000). Now, we have asked whether Met^{d} could still convey a residual signal through Gab1.

Figure 1 shows that Met^{d} could no longer bind Gab1 ([B], left), or Grb2, Src, and p85PI3K ([B], right; Ponzetto et al., 1994; Bardelli et al., 1999), and caused reduced Gab1 phosphorylation (C), lower Ras activation (D), and ERK/MAPK phosphorylation (E) in hepatocyte cultures. The same was also true for Akt/PKB (Figure 1E), whose

upstream activator p85PI3K can be recruited by Gab1 (Holgado-Madruga et al., 1997). Thus, Met^{d} indeed conveys a residual signal via Gab1. However, the lethal phenotype of *met$^{d/d}$* mutants (Maina et al., 1996) shows that the signal is below threshold in vivo.

Generation of Mutant Mice with Met Receptors Displaying Enhanced Recruitment of Specific Effectors

We generated *met* specificity-switch mutants to superimpose a specific pathway on the background of Gab1-mediated signaling. To selectively recruit PI-3 kinase or Src, the two Met multifunctional tyrosines were converted into optimal motifs for p85 (Y_{1349}MDMSATY$_{1356}$MDMS; *met^{2P}*) or for Src (Y_{1349}EEINATY$_{1356}$EEI; *met^{2S}*; Songyang et al., 1993; Figure 2A). To enhance signaling through Grb2, Y_{1349} was converted into a second Grb2 binding site (Y_{1349}VNVNATY$_{1356}$VNV; *met^{2G}* allele; Figure 2A). The *neo* cassette was flanked by *LoxP* sites (Figure 2A) to allow excision by crossing mutant mice with the *Cre Deleter* strain (Schwenk et al., 1995) (Figure 2C). The *neo* cassette caused a slight reduction in the expression of the chimeric receptor in some tissues (Figure 2D). All data presented here were from *met* alleles lacking the *neo* cassette.

Expression and activity of the specificity-switch mutants were assayed in cultures of hepatocytes from E15.5 homozygous mutant embryos. Figure 2E shows that an equal level of Met protein was present in all mutant hepatocytes, while mildly reduced levels of Met^{d} protein were expressed by the *met^{d} neo+* allele. Thus, the knockin mutants previously described (all neo +; Maina et al., 1996) should be interpreted as a "sensitized" model where the effects of the signaling mutations may in some tissues have been enhanced by a reduced amount of the receptor. Upon HGF stimulation, all Met mutants became equally phosphorylated in vivo (Figure 2F) and displayed similar in vitro kinase activity toward an exogenous substrate (Figure 2G). Thus, the new mutations did not affect the ability of the Met receptor to carry out auto- or transphosphorylation.

To analyze the interactions of the mutant Met receptors with signaling proteins in vitro, GST-fusion proteins of the SH2 domains of p85PI3K and Src, or full-length Grb2 were used in pull-down experiments. Activated Met^{2P} was able to associate with the p85PI3K C-terminal SH2 domain, but not with the Src SH2 domains or with Grb2 (Figure 3A). In contrast, Met^{2S} was pulled down by the Src SH2 domain, but not by that of p85PI3K or by Grb2 (Figure 3A). Two optimal binding sites for Grb2 (Met^{2G}) allowed binding with Grb2, p85PI3K, and Src, similar to the wild-type receptor (Figure 3A). Next, we asked whether mutant Met receptors interacted selectively with effectors in vivo. Upon HGF stimulation, endogenous p85PI3K and Grb2 coimmunoprecipitated with the Met^{2P} and Met^{2G} mutants, respectively, but not with the Met^{2S} receptor (Figure 3B). PI3K activity associated with Met^{2P} was enhanced relative to Met^{2S} and Met^{2G} immunoprecipitates (Figure 3C; Bardelli et al., 1999). We were unable to demonstrate Src binding to the Met^{2S} receptor in vivo, most likely because of the lack of sensitivity of the anti-Src antibodies. We detected, however, HGF-induced tyrosine phosphorylation of endogenous Src in primary *met$^{2S/2S}$* and *met$^{2G/2G}$*, but not in *met$^{2P/2P}$* hepatocytes (Figure 3D). These findings provide compelling evidence that in Met^{2P} and Met^{2S} receptors the docking sites were effectively converted from multifunctional to specific for PI3K and Src.

Signaling via Gab1 Is Unaltered Downstream of Met Specificity-Switch Mutants

Since changes in Gab1 signaling would have to be taken into account when interpreting the phenotypes of the Met specificity-switch mutants, we checked whether the presence of specific binding motifs could interfere with Gab1 binding and signaling.

We first checked whether Met mutants could interact with the Gab1 MBD in vitro. Contrary to Met^{d}, the GST-MBD of Gab1 pulled down Met equally well from lysates of wild-type and mutant hepatocytes. Only binding with Met^{2P} was reproducibly weaker (Figure 4A). In vivo binding with Gab1 could not be verified, either because the level of bound Gab1 was too low, or because the anti-Gab1 antibodies were not sensitive enough. HGF-induced Gab1 phosphorylation was similar in mutant and wild-type cells (Figure 4B). We thus tested the ability of Gab1 to recruit effectors in vivo upon HGF stimulation of mutant and wild-type hepatocytes. Gab1 interacted with p85PI3K and Grb2 equally well in all cells (Figure 4C). The PI3K activity associated with Gab1 was also the same in mutant and control hepatocytes (Figure 4D). In conclusion, all mutants retained Gab1-mediated signaling to the same extent. Therefore, phenotypic changes observed in *met* mutant mice should not be due to altered Gab1 signaling, but rather to differential coupling of Met with effectors.

Overall Signaling Potential of Met Specificity-Switch Mutants

We next investigated the overall effect of the mutations on downstream targets. These downstream modifications are likely to represent the sum of Gab1-mediated and direct Met signaling. To assess the ability of wild-type and mutant Met receptors to activate PI3K, we analyzed its activity in anti-phosphotyrosine immunoprecipitates (α-pY, including Met and Gab1) obtained from HGF-stimulated hepatocytes. PI3K activity was similar in wild-type, Met^{2G}, and Met^{2P} hepatocytes but was markedly reduced in Met^{2S}-expressing cells (Figure 5A).

HGF stimulation caused sustained phosphorylation of Akt only in wild-type and Met^{2G} hepatocytes (Figure 5C, middle). The specific PI3K inhibitor LY294002 blocked Akt phosphorylation in all cultures, indicating that PI3K activity is necessary for Akt activation. Surprisingly, however, the levels of phospho-Akt downstream of Met^{2P} were reduced to the same extent as downstream of Met^{2S} (Figure 5C). This suggests that other Met effectors (besides PI3K and Gab1) must contribute to this activation.

We next studied the ability of wild-type and Met signaling mutants to activate the Ras/Raf/Mek/ERK pathway, by measuring Ras-GTP using a GST-fusion protein of the Raf Ras binding domain (RBD). Met^{2P} and Met^{2S} led to reduced levels of activated Ras compared to wild-type Met or Met^{2G} (Figure 5B). We also analyzed HGF-induced ERK1 and ERK2 phosphorylation. ERK phos-

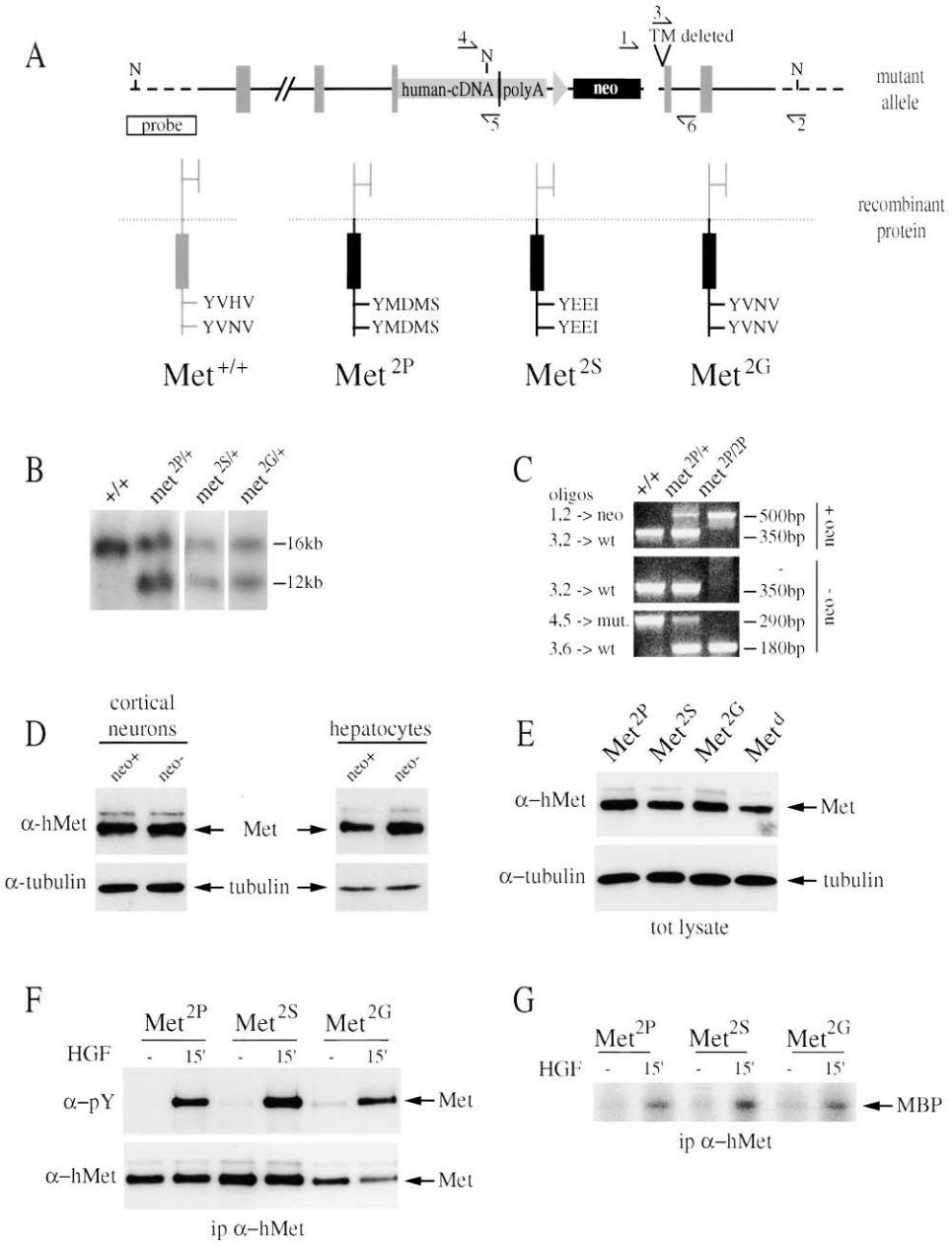

Figure 2. Knockin of Specificity-Switch Mutations in the *met* Locus and the Expression and Activity of Recombinant Met Protein in Primary Cultures

(A) Scheme of mutant alleles and of chimeric Met protein products. The knockin strategy was previously described (Maina et al., 1996). Boxes represent exons. N indicates NdeI sites. The *neo* cassette was flanked by loxP sites (triangles). Numbered arrows indicate oligonucleotide primers used for genotyping neo+ and neo− alleles. The knocked-in human cDNA fragment codes for the transmembrane and cytoplasmic domains of the Met receptor (black). $Met^{+/+}$: mouse Met receptor. Met^{2P}, Met^{2S}, and Met^{2G}: chimeric receptors with two optimal binding sites for PI3K, Src, or Grb2.

(B) Southern blot analysis of NdeI digests of genomic DNA isolated from R1 ES cell controls, or double selected ES cell clones, electroporated with met^{2P}, met^{2S}, and met^{2G} constructs. The probe used (shown in [A]) identifies a 16 kb NdeI DNA fragment in the +/+ allele, and a 12 kb NdeI fragment in the recombinant alleles.

(C) PCR analysis of genomic DNA showing the removal of the *neo* cassette by Cre-mediated excision (see Experimental Procedures).

(D) Comparison of the level of recombinant Met^{2G} protein produced before and after excision of the *neo* cassette. Met was visualized in Western blots of lysates of cortical neurons and hepatocytes, derived from neo+ and neo− Met^{2G} E15.5 embryos. The blots were reprobed with α-tubulin antibodies as a control for the amount of protein in the lysates.

(E) Levels of recombinant Met protein in specificity-switch mutants. Western blots of total protein from mutant hepatocytes were probed with α-hMet. The blot was reprobed with α-tubulin as a control. Note that the level of Met^{d} is reduced by the *neo* cassette. Therefore $met^{WT/WT}$ hepatocytes were used as positive control for $met^{d/d}$ (neo+), and wild-type hepatocytes (+/+) as a positive control for the *met* specificity-switch mutants (neo−).

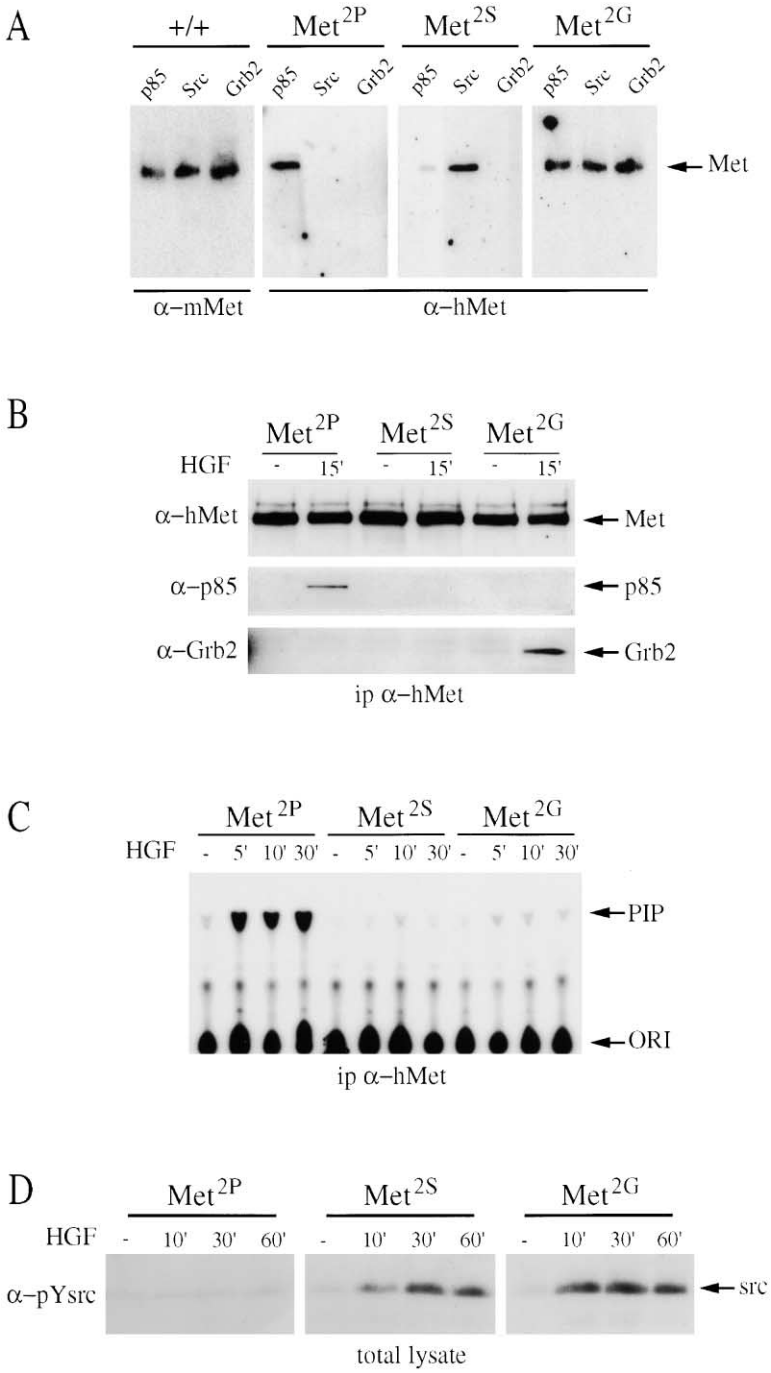

Figure 3. Interaction of Specificity-Switch Mutants with Signaling Proteins

(A) In vitro association of Met specificity-switch mutants with the SH2 domains of p85, Src, and Grb2. GST-fusion proteins of SH2 domains were immobilized on glutathione-Sepharose and incubated with lysates from HGF-stimulated wild-type (+/+) and mutant hepatocytes. The complexes were blotted and probed with α-mouse-Met (α-mMet) for wild-type embryos, or α-hMet for mutant embryos.

(B) HGF-induced binding of Met specificity-switch mutants with endogenous p85 and Grb2. Met was immunoprecipitated from mutant hepatocytes. Coimmunoprecipitated p85 and Grb2 were visualized by Western blot with specific antibodies. α-hMet was used to assess the level of Met protein in the lysates.

(C) Time course of HGF-induced PI3K activity associated to Met specificity-switch mutants. PI3K assays were carried out on α-hMet immunoprecipitations obtained from mutant hepatocytes. Control samples from *met*$^{+/+}$ hepatocytes could not be included in (B and C) because the α-mMet antibodies are inefficient in immunoprecipitations.

(D) Time course of HGF-induced Src phosphorylation by Met specificity-switch mutants. Lysates of mutant hepatocytes were blotted and probed with phospho-Src antibodies.

phorylation was equivalent and sustained for 60 min in wild-type and *met*$^{2G/2G}$ hepatocytes (Figure 5C). In contrast, phospho-ERKs were reduced in *met*$^{2P/2P}$ and *met*$^{2S/2S}$ hepatocytes (Figure 5C), correlating with reduced levels of Ras-GTP in these cultures. LY294002 had no effect on this pathway.

Altogether, the results of the biochemical analysis described above show that following HGF stimulation (1) Met^{d} maintains the ability to activate (via Gab1) a subthreshold of PI3K/Akt and Ras/ERK pathways, (2) specificity-switch mutants fully retain Gab1 signaling, (3) Met^{2P} and Met^{2S} recruit and activate, respectively, PI3K

(F) HGF-induced phosphorylation of Met specificity-switch mutants. Lysates of hepatocytes, either untreated or HGF-stimulated were immunoprecipitated with α-hMet, blotted and probed with α-pY, and reprobed with α-hMet antibodies.

(G) Kinase activity of Met specificity-switch mutants on an exogenous substrate. Met IPs were incubated with [γ-^{32}P]ATP and MBP as exogenous substrate. The amount of Met in the lysates is shown in (F), bottom.

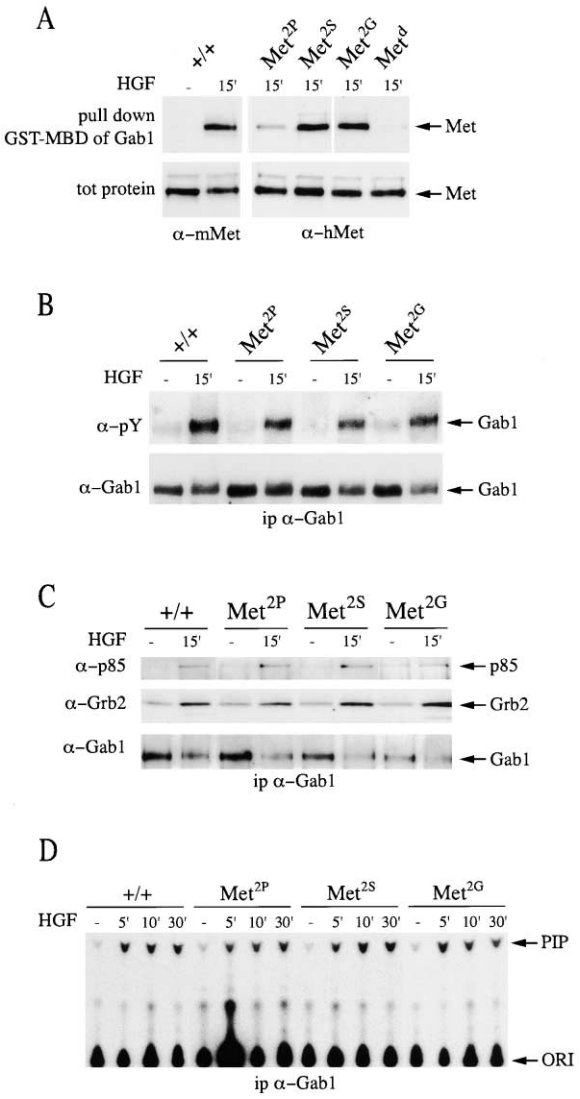

Figure 4. Analysis of Gab1 Signaling Downstream of Met Specificity-Switch Mutants

(A) In vitro binding of Gab1 MBD with wild-type Met (+/+) and Met specificity-switch mutants. A GST-fusion protein of the Gab1 MBD was immobilized on glutathione-Sepharose and incubated with lysates from untreated or HGF-stimulated wild-type (+/+) and mutant hepatocytes. Complexes were blotted and probed with α-mMet or α-hMet antibodies (for wild-type or mutant samples). The amount of Met used is shown in Western blots of total proteins (bottom).

(B) HGF-induced Gab1 phosphorylation in wild-type and Met specificity-switch mutants. Gab1 was immunoprecipitated from lysates of untreated or HGF-stimulated wild-type (+/+) and mutant hepatocytes. Immunoprecipitations were blotted and probed with α-pY antibodies and reprobed with α-Gab1 antibodies.

(C) HGF-induced binding of effectors to Gab1 downstream of wild-type Met and Met specificity-switch mutants. Gab1 molecules were immunoprecipitated from lysates of untreated or HGF-stimulated wild-type (+/+) and mutant hepatocytes. Coimmunoprecipitated signaling molecules were visualized by Western blot with α-p85 and α-Grb2 antibodies. Blots were reprobed with α-Gab1 antibodies as a control for Gab1 level.

(D) Time course of HGF-induced PI3K activity associated with Gab1 downstream of wild-type and Met specificity-switch mutants. PI3K assays were carried out on α-Gab1 immunoprecipitations obtained from lysates of unstimulated or HGF-treated wild-type (+/+) or mutant hepatocytes.

and Src, and (4) Met^{2P} and Met^{2S} show reduced downstream activation of ERKs and Akt. The main questions left open were: are Met-mediated biological functions fully restored by the specificity-switch mutants, since the signal capacity of the adaptor Gab1 seems to be intact? Or, given their lower threshold of overall signaling, would targeted expression of Met^{2P} and Met^{2S} produce similar hypomorphic phenotypes in vivo? Alternatively, would these signaling mutations lead to qualitatively different phenotypes?

Selective PI3K or Src Docking Sites in Met Are Not Sufficient to Promote Hepatocyte Survival In Vivo

Embryonic liver is defective in met^{d} embryos, as in *hgf* and *met* null mutants (reviewed in Birchmeier and Gherardi 1998). To avoid indirect effects due to defective placental development, which also depends on Met, we backcrossed the new mutants into the outbred strain CD1. In this mixed strain (F1 CD1), the placental defect is partially rescued, and lethality is delayed past E15.5 even in the most severe met^{d} mutant (data not shown). While the body weight of $met^{2P/2P}$ and $met^{2S/2S}$ mutant embryos at E15.5 was only mildly reduced (15%–20%), liver weight was reduced by 60% and 55% compared to control and $met^{2G/2G}$ embryos, similar to the most severe $met^{d/d}$ mutants (Figures 6A–6C and 6J). Histology on E14.5 liver sections revealed that while the liver of $met^{2G/2G}$ and wild-type embryos were indistinguishable (Figure 6F and data not shown) in $met^{2P/2P}$ and $met^{2S/2S}$ mutants, the liver structure was loose, with enlarged sinusoidal spaces and dissociated parenchymal cells, similar to that of *hgf* nulls (Figures 6D and 6E).

We then asked whether hepatocyte survival was affected in mutant embryos. At E12.5, 2 days before the reduction in liver size became apparent, TUNEL-positive cells were increased by 4- to 5-fold in the liver section of $met^{2P/2P}$ and $met^{2S/2S}$ mutants relative to wild-type and $met^{2G/2G}$ embryos (Figures 6G–6I and 6K). This increase was comparable to that seen in the $met^{d/d}$ mutants (Figure 6K). Other tissues that do not express Met did not display an increase in apoptotic cells (data not shown), confirming that the defect was due to insufficient Met signaling in hepatocytes rather than to poor embryo survival. Furthermore, the fact that placental development was rescued in $met^{2S/2S}$ mutants (see Figure 7) argues strongly against the liver defect being secondary to placental malfunction. These results indicate that signaling through effectors other than PI3K or Src is required for Met-mediated hepatocyte survival.

Selective Src, But Not PI3K, Docking Sites in Met Are Sufficient for Normal Placental Development and Fetal Myoblast Proliferation

Embryos lacking either HGF or Met die during embryogenesis because of defective placental development (reviewed in Birchmeier and Gherardi, 1998), similar to met^{d} mutants (Maina et al., 1996). Met seems to be necessary for the growth of trophoblast cells. A Met receptor with either two Src (met^{2S}) or two Grb2 (met^{2G}) binding sites was sufficient for placental development and to bypass embryonic lethality (Figures 7B and 7C). While $met^{2G/2G}$ mice were viable, fertile, and indistinguishable from controls, $met^{2S/2S}$ mutants were born alive but

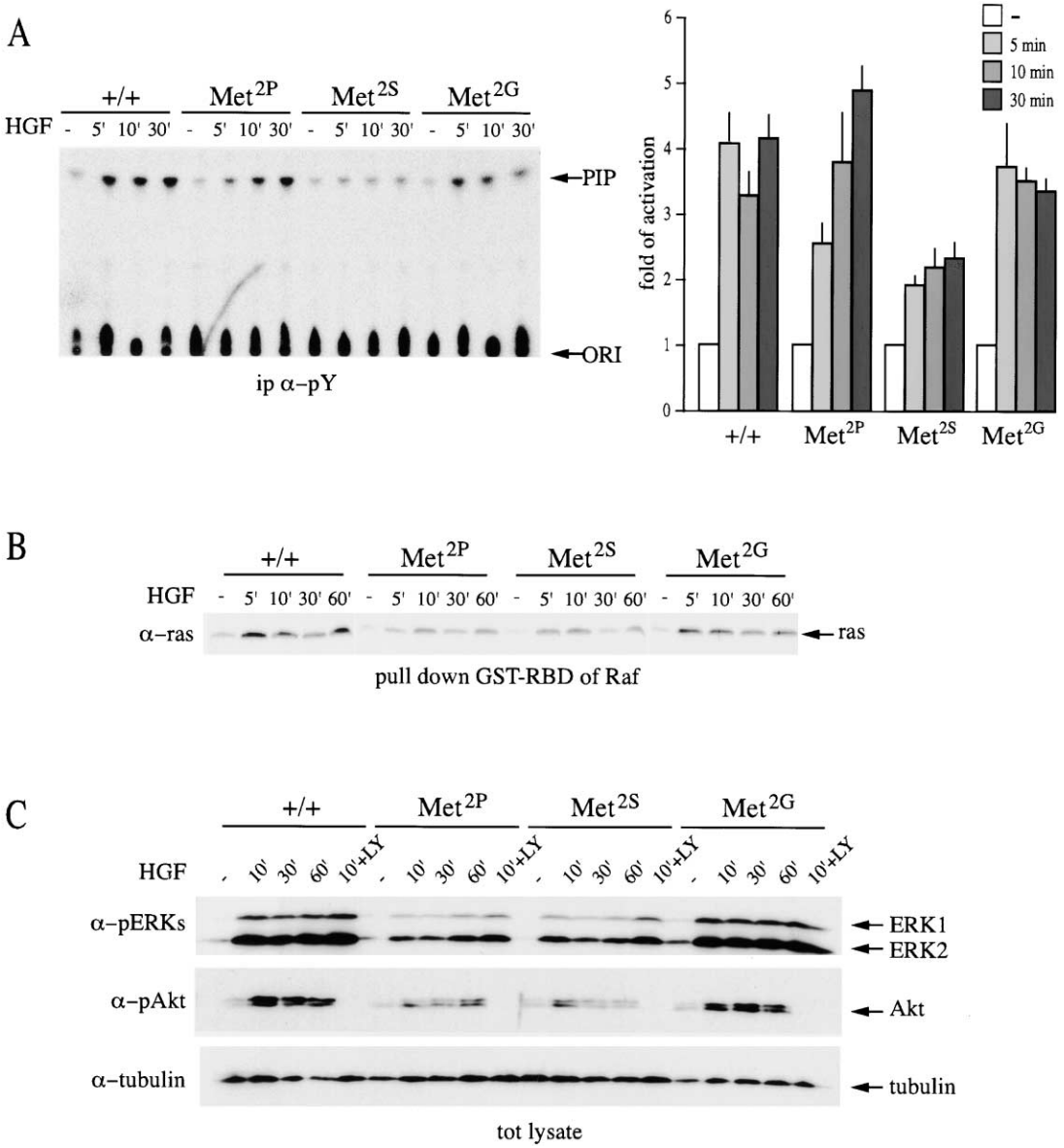

Figure 5. Activation of PI3K and Ras Downstream of Met Specificity-Switch Mutants

(A) Time course of HGF-induced PI3K activity associated with phosphoproteins. PI3K assays were carried out on α-pY IPs obtained from the lysates of untreated or HGF-stimulated hepatocytes. Bars in the graph on the right represent the mean of three independent experiments.

(B) Time course of HGF-induced Ras activation in wild-type and mutant hepatocytes. A GST-fusion protein of the Raf RBD was immobilized on glutathione-Sepharose and incubated with lysates from wild-type (+/+) and mutant hepatocytes. Complexes were blotted and probed using α-Ras antibodies.

(C) Time course of HGF-induced ERK and Akt phosphorylation in wild-type and mutant hepatocytes. Extracts were blotted and probed with phospho-ERK (α-pERKs, top) or Akt (α-pAkt, middle) antibodies, and reprobed with α-tubulin. The PI3K-specific inhibitor LY294002 (LY) selectively blocked Akt but not ERK phosphorylation.

died immediately after birth of respiratory failure due to severe reduction of the diaphragm. Specific PI3K binding sites were not sufficient for normal placental development. Beginning at around E13.5 and becoming more evident in the next two days, the placenta of the *met*$^{2P/2P}$ mutants appeared paler and smaller than controls (Figure 7A), and led to the lethality of the embryos between E13.5 and E15.5. These results indicate that Met-mediated Src activation is sufficient for placental development and suggest a role for Src in promoting trophoblast proliferation.

We next turned to fetal myoblasts, a subpopulation of myoblasts that comes out of quiescence at the onset of secondary myogenesis (E14), and whose proliferation depends on Met signaling (Maina et al., 1996). Pregnant females were injected twice with BrdU at E15 and E15.5, and were sacrificed at E17.5. BrdU-labeled nuclei located underneath the basal lamina were counted on

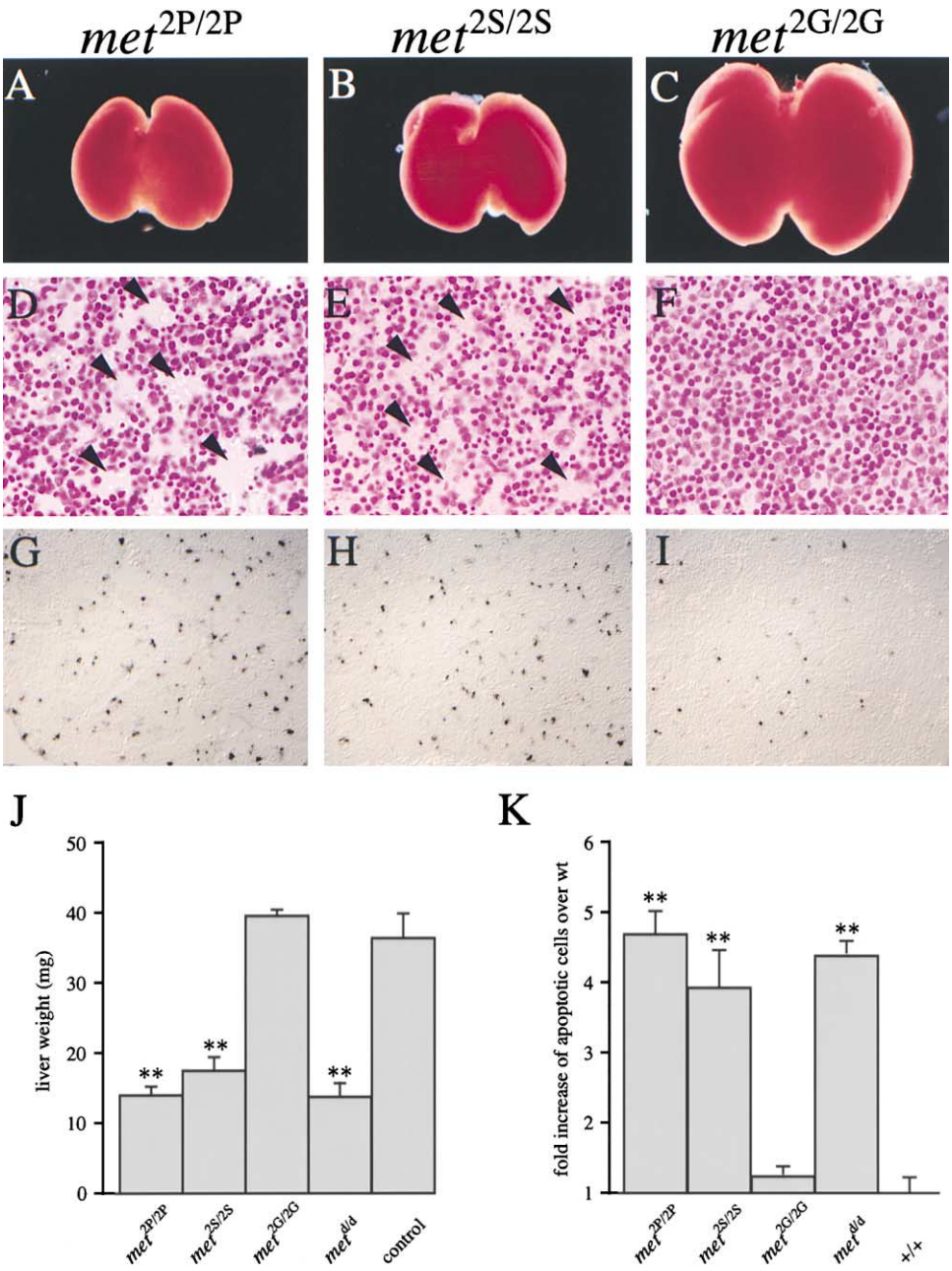

Figure 6. Selective p85 or Src Binding Sites in the Met Receptor Are Not Sufficient for Liver Development

(A–C) Freshly dissected liver from E15.5 homozygous mutant embryos.

(D–F) Feulgen-stained liver sections from E14.5 mutant embryos. Arrowheads indicate enlarged sinusoidal spaces.

(G–I) TUNEL staining of paraffin liver sections from E12.5 mutant embryos.

(J) Quantitative analysis of liver mass of E15.5 homozygous *met* mutant embryos and controls (**: P values < 0.0001, t tests).

(K) Quantitative analysis of TUNEL-positive nuclei in E12.5 mutant and wild-type liver sections (**: P values < 0.0001, t tests). Magnifications are 400× (D–F) and 100× (G–I).

sections of intercostal muscles double stained for BrdU and laminin. We found a 55% reduction in the number of BrdU-positive myogenic nuclei in homozygous $met^{2P/2P}$ mutants compared to wild-type controls, similar to $met^{d/d}$ embryos (Figure 7G). In contrast, fetal myoblast proliferation was completely rescued in homozygous $met^{2S/2S}$ and $met^{2G/2G}$ mutants (Figure 7G).

The proliferative response of fetal myoblasts to HGF was also evaluated in vitro, using primary fetal myoblasts isolated from back muscle of E14.5 control and mutant embryos (Figure 7D–7F and 7H). HGF increased the number of BrdU-positive wild-type fetal myoblasts by approximately 30%. This effect was comparable to that obtained using 0.5% chicken embryo extract (CEE; Figure 7H). Similar results were obtained with cells derived from $met^{2G/2G}$ and $met^{2S/2S}$ embryos (Figures 7E, 7F,

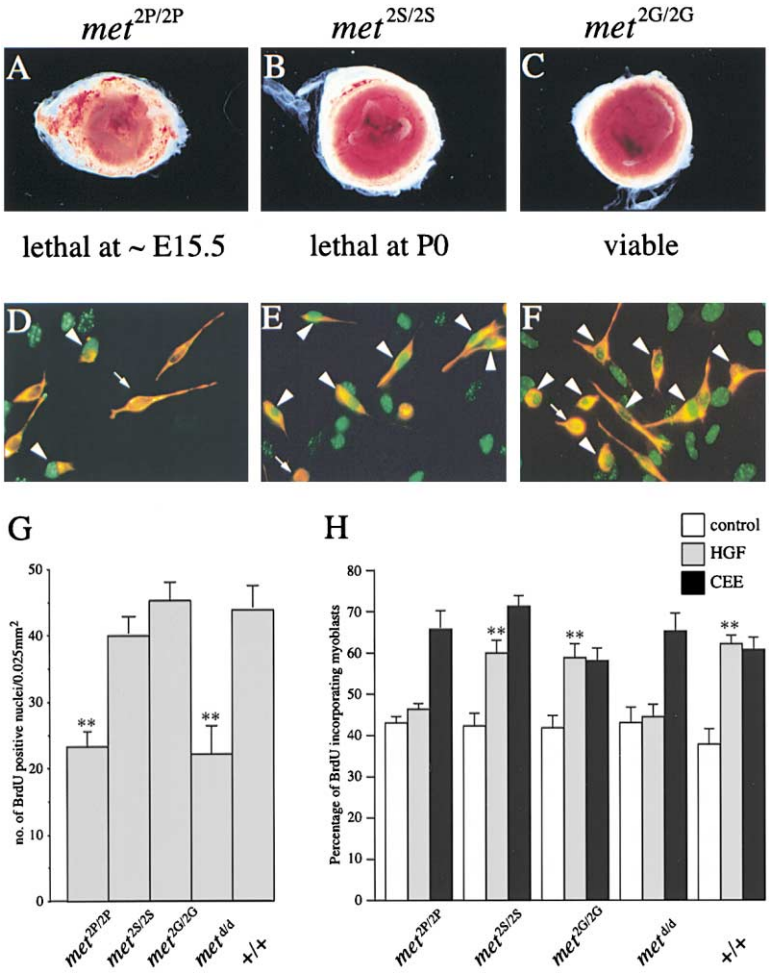

Figure 7. Selective Src (But Not PI3K) Binding Sites in Met Are Sufficient for Placental Development and Fetal Myoblast Proliferation

(A–C) Morphology of freshly dissected E13.5 placenta.

(D–F) E14.5 primary myoblasts from *met* mutant embryos treated with HGF (10 ng/ml), and double stained with α-desmin (red) and α-BrdU (green). Arrowheads show proliferating myoblasts (desmin/BrdU-positive). Arrows show quiescent myoblasts (desmin-positive/BrdU-negative). Magnification is 400×.

(G) Quantitative analysis of BrdU-labeled nuclei in intercostal muscle of E17.5 embryos (see Maina et al., 1996). **: P values < 0.0001, t tests.

(H) Quantitative analysis of proliferating fetal myoblasts cultured without additives (control), with HGF, or with chicken embryo extract (CEE). Bars are the mean of three separate experiments. 3–4 embryos/genotype were pooled in each culture. **: P values < 0.0001, t tests.

and 7H). $met^{2P/2P}$ fetal myoblasts failed to respond to HGF, similar to $met^{d/d}$ cells (Figures 7D and 7H). $met^{2P/2P}$ myoblasts responded normally to CEE, confirming that the defect was specific for HGF. Together with the rescue of placental development, these results suggest that Src, but not PI3K, is a mediator of HGF-induced myoblast and trophoblast proliferation.

Neither Src nor PI3K Docking Sites in Met Are Sufficient to Promote Full Myoblast Migration

In *hgf* or *met* null mutants, or in met^{d} embryos, embryonal myoblasts fail to delaminate from the somites and to undergo long-range migration (reviewed in Birchmeier and Gherardi, 1998). Thus, the limbs of these mutants are devoid of muscle. In situ hybridization on E10.5 embryos with a *met* probe showed that in $met^{2P/2P}$ and $met^{2S/2S}$ mutants, very few myogenic precursors migrate out of the somites. In contrast, in $met^{2G/2G}$ embryos, all myoblast precursors delaminate from the limb somites resulting in a diffuse staining pattern identical to controls (Figure 8A–8D and data not shown). In situ hybridization with a *MyoD* probe at E13.5 revealed a severe reduction of the muscle mass in the limbs of both $met^{2P/2P}$ and $met^{2S/2S}$ mutants (Figures 8E and 8F). $met^{2G/2G}$ embryos were identical to wild-type controls (Figure 8G and data not shown), while $met^{d/d}$ mutants were completely devoid of limb muscles (Figure 8H). The muscle defect was further characterized by measuring the muscle area on transverse sections of E15.5 forelimbs in the proximal part. The muscle masses of $met^{2P/2P}$ and $met^{2S/2S}$ embryos were reduced to approximately 40%, compared to wild-type control and $met^{2G/2G}$ embryos (Figures 8I–8L and 8Q). A drastic reduction was also observed in the diaphragm muscle of both $met^{2P/2P}$ and $met^{2S/2S}$ mutants. The diaphragm is also formed by migratory myoblast precursors, and thus it was normal in $met^{2G/2G}$ embryos but absent in $met^{d/d}$ embryos (Figures 8O and 8P). These results clearly indicate that neither PI3K nor Src docking sites in Met are sufficient to promote full migration of myoblast precursors, and suggest that a more complex signaling output is required for this process.

Selective PI3K, But Not Src, Docking Sites in Met Are Sufficient for Axon Outgrowth and Branching In Vivo

Recently it was shown that HGF induces axon outgrowth and branching in different neuronal cells (reviewed in Maina and Klein, 1999; see Caton et al., 2000). In the developing limbs of *hgf* and met^{d} mutant embryos, certain motor nerves showed outgrowth and fasciculation defects as they emerged from a normally formed brachial plexus. We analyzed nerve development in mutant embryos by whole-mount antineurofilament staining,

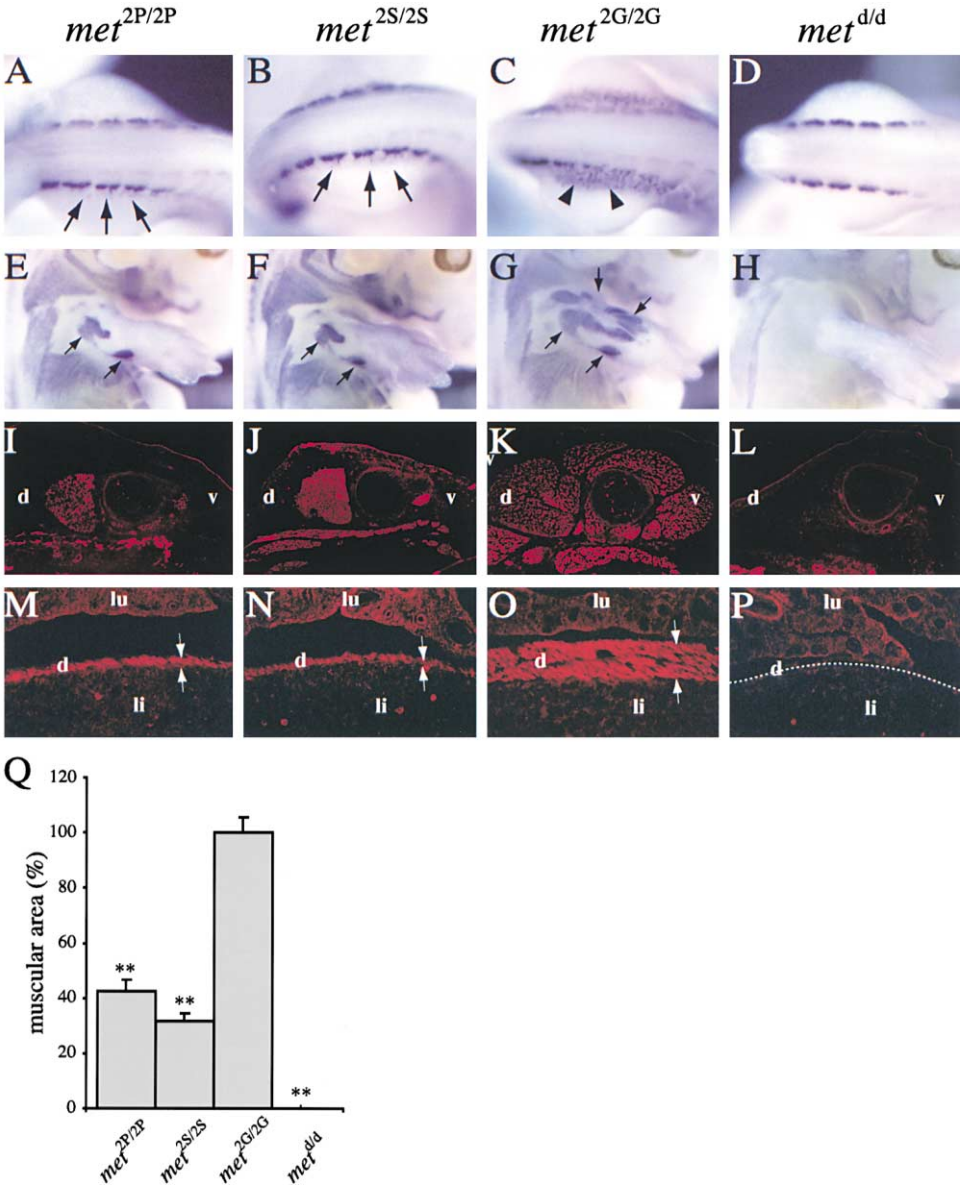

Figure 8. Selective p85 or Src Binding Sites in Met Are Insufficient for Full Migration of Myoblast Precursors

(A–D) Whole-mount in situ hybridization of E10.5 embryos with a *met* probe. Arrows in (A and B) indicate rare migrating myoblasts in $met^{2P/2P}$ and $met^{2S/2S}$ mutants. Arrowheads in (C) indicate a normal pattern of migrating myoblast precursors in $met^{2G/2G}$ embryos. In $met^{d/d}$ embryos, myoblasts do not delaminate from the somite (D).

(E–H) Whole-mount in situ hybridization of E13.5 embryos with a *MyoD* probe. Arrows indicate the forming muscles in the forelimb.

(I–L) Proximal forelimb sections of E15.5 mutant embryos, stained with phalloidin. d: dorsal muscles; v: ventral muscle

(M–P) Section of the diaphragm stained with phalloidin. In the $met^{d/d}$ mutants, a stippled line indicates the position where the diaphragm should be. lu: lung; d: diaphragm; li: liver. Magnification is 50× in (I–L) and 200× in (M–P).

(Q) Quantitative analysis of muscle mass in E15.5 homozygous *met* mutant embryos and controls (**: P values < 0.0001, t tests).

and by crossing mutant mice with a transgenic line expressing the *LacZ* gene under the *Hoxa-7* promoter (Tremblay et al., 1995). Selective PI3K docking sites in Met are sufficient to promote the outgrowth of motor axons (Figures 9A, 9D, and 9H). In fact, in $met^{2P/2P}$ embryos, the pattern of limb nerves was nearly comparable to that seen in $met^{2G/2G}$ embryos (Figures 9C, 9F, and 9J), and in turn indistinguishable from controls (data not shown). In contrast, motor axon outgrowth in $met^{2S/2S}$ mutant limbs was defective (Figures 9B, 9E, and 9I) and comparable to that of $met^{d/d}$ mutants (Maina et al., 1997). In particular, branches of *Nervus thoracodorsalis* were indistinguishable from the control in $met^{2P/2P}$ and $met^{2G/2G}$ embryos, whereas they were completely absent in $met^{2S/2S}$ mutants (compare Figures 9D and 9F with 9E). β-Galactosidase staining in mice carrying the *Hoxa-7 LacZ* transgene confirmed the presence of the *Nervus thoracodorsalis* only in $met^{2P/2P}$, but not in $met^{2S/2S}$ mutants (Figure 9G–9J). The motor nerve defect was also rescued in the hind limbs of $met^{2P/2P}$ embryos (data not shown). However, more anterior nerves in $met^{2P/2P}$ embryos were defective, as in $met^{2S/2S}$ mutants. Together,

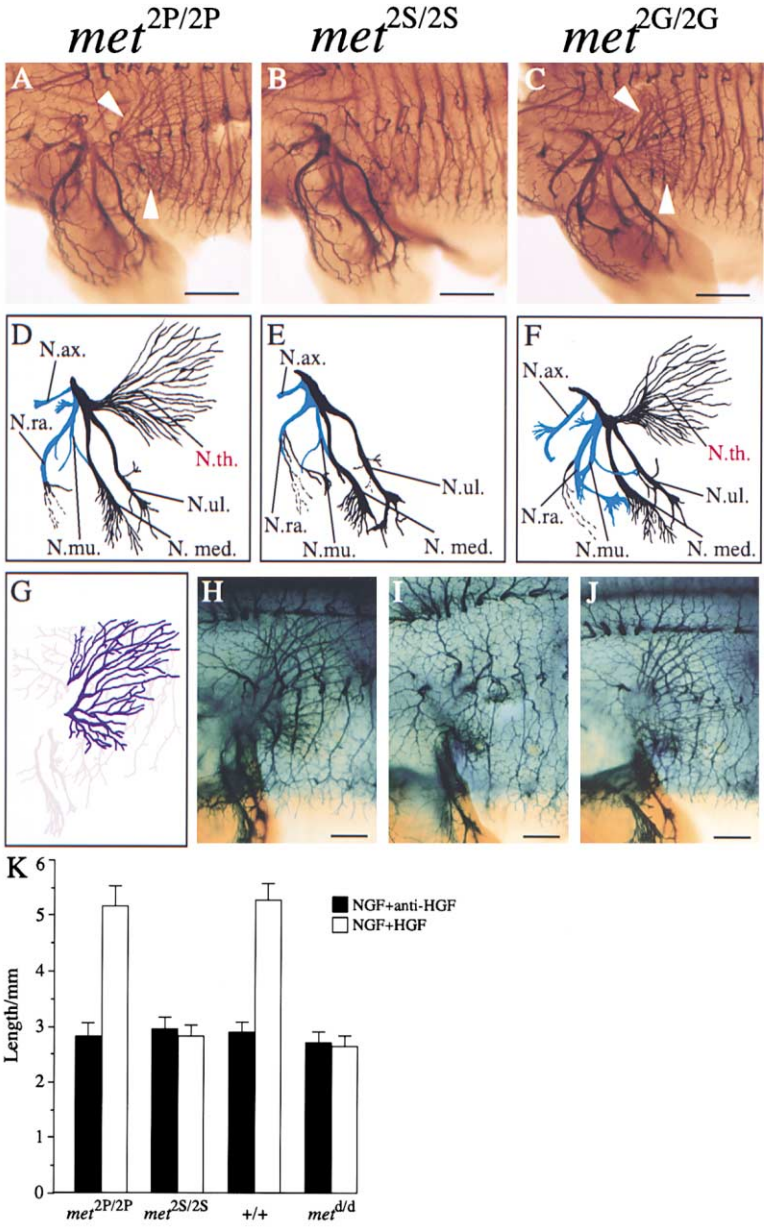

Figure 9. Selective p85 (But Not Src) Binding Sites in Met Are Sufficient for Axon Outgrowth

(A–C) Whole-mount antineurofilament staining of E12.5 embryos (forelimb and thorax; dorsal up, anterior left). Arrowheads indicate branches of *Nervus thoracodorsalis.* Scale bar is 0.6 mm.

(D–F) Scheme of forelimb nerves. *Nervus Thoracodorsalis* (N. th.), (N. med.) Nervus medianus (N. ul.) Nervus ulnaris. *Nervus axillaris* (N. ax.), *Nervus radialis* (N. ra.), *Nervus musculocutaneous* (N.Mu.), indicated in blue, are reduced in $met^{2P/2P}$ and $met^{2S/2S}$ relative to $met^{2G/2G}$ mutants. Sensory nerves emerging from the *Nervus radialis* are not drawn in detail.

(G) Drawing of limb nerves stained for β-gal in (H). *Nervus thoracodorsalis*is is highlighted in blue.

(H–J) β-gal staining of *met* mutant embryos carrying a LacZ transgene under the *Hoxa-7* promoter. Scale bar is 0.4 mm.

(K) Quantitative analysis of sympathetic neuron axon outgrowth in vitro. Superior cervical ganglia (SCG) from E14.5 embryos were dissociated, trypsinized, and cultured with either NGF and neutralizing HGF antibodies, or NGF and HGF.

these results show that selective PI3K docking sites in Met are sufficient to promote outgrowth of specific motor axons in vivo.

Selective PI3K Docking Sites in Met Are Sufficient for Axon Outgrowth In Vitro

Having observed a requirement for PI3K signaling downstream of Met for motor axon outgrowth in vivo, we sought corroborating evidence from in vitro studies. We had previously shown that HGF and nerve growth factor (NGF) cooperate in promoting axon outgrowth in cultures of superior cervical ganglion (SCG) sympathetic neurons (Maina et al., 1998). We therefore established SCG neuron cultures from E14.5 wild-type and *met* mutant embryos, and monitored neurite growth of individual neurons in the presence of NGF plus neutralizing anti-HGF antibodies, and NGF plus HGF. Because HGF has multiple effects on sympathetic neurons, serial drawings were made of the same neurons between 3 and 48 hr, and only neurons that survived throughout this period were included in the analysis. Neurite arbors of $met^{2P/2P}$ SCG neurons were significantly greater with NGF plus HGF than in the presence of NGF plus anti-HGF, on average 2-fold longer, similar to wild-type neurons (Figure 9K and data not shown). In contrast, HGF did not significantly enhance the size of neurite arbors of SCG neurons from $met^{2S/2S}$ embryos (Figure 9K). These results show that HGF/Met signaling through PI3K plays a crucial role in enhancing the overall length of sympathetic neurite arbors, while signaling via Src is not sufficient for neurite outgrowth.

Discussion

Understanding growth factor receptor signal transduction has been a major achievement in the last decade.

The discovery that each receptor is endowed with an individual signaling profile conferred by its docking sites suggested at first that specific biological responses could derive from the activation of different signaling pathways, which in turn could elicit specific transcriptional programs. It has, however, become evident that cross talk between pathways occurs distal to the receptor, prompting the question: do all roads lead to the activation of the same genes? And, if so, where does the specificity lie? (Pawson and Saxton, 1999). Recent experiments with add-back mutants of the PDGF receptor suggest that diverse biological responses may result from quantitative rather than qualitative differences in downstream signaling, and that only a minority of genes may operate through a pathway-specific transcriptional response (Fambrough et al., 1999). Since minor differences in gene expression can result in dramatically different developmental programs, the effects of signaling mutants are better appreciated by testing them in vivo. In the present work, we have described *met* mutant mice where we switched toward PI3K, Src, or Grb2 the specificity of the multifunctional tyrosines responsible for signaling.

To interpret the phenotype of the new animal models, we needed to characterize the Met mutants in terms of their downstream signaling. In particular, it was important to establish whether the specificity-switch mutants could still bind and phosphorylate Gab1. Gab1 is not an exclusive substrate for Met, since insulin, EGF, PDGF, and neurotrophin receptors can also phosphorylate it. The phenotype of Gab1 knockout mice suggests that Gab1 may indeed play an essential role downstream of Met and all of these receptors (Itoh et al., 2000; Sachs et al., 2000). We first went back to the severe "loss-of-function" mouse model, met^{d}, where the two docking sites were abrogated by Tyr → Phe substitutions. HGF stimulation of primary hepatocytes showed that the Met^{d} receptor could no longer bind, but could still transphosphorylate Gab1, although to a lower level with respect to Met^{WT}. Accordingly, in these cells there was a residual low threshold of activation of Ras and PI3K targets in response to HGF. Thus, the Met^{d} receptor is not truly signaling dead. The same kind of analysis was extended to hepatocytes from the new mutants. Gab1 could still bind all the Met specificity-switch mutants in vitro. The interaction was weaker only with Met^{2P}. More importantly, in primary cells, all three Met mutants responded to HGF by phosphorylating Gab1 at a level indistinguishable from wild-type. A limit of our analysis is that we used only hepatocytes, and a concentration of ligand, which may be higher than physiological. It is possible that in cells expressing low levels of the multiadaptor, and especially in the case of the Met^{2P} mutants, Gab1 phosphorylation may be reduced. However, in cultured hepatocytes, HGF-induced binding of PI3K and Grb2 to Gab1, and Gab1-associated PI3K activity, were the same for all mutants and comparable to wild-type. These results indicate that all specificity-switch Met mutants retained the ability to signal through Gab1. Thus, phenotypic differences in the mutant mice should not be attributed to altered Gab1 phosphorylation, but rather to differential recruitment of effectors.

Met^{2P} and Met^{2S} showed lower overall HGF-induced activation of Ras/MAPK and Akt with respect to wild-type and Met^{2G}. We were surprised to find decreased activation of Akt, a known PI3K target, downstream of the Met^{2P} mutant, since PI3K activity associated with Met^{2P} was higher than in controls. Our data suggest that additional signals may be necessary to evoke full Akt activation.

Our analysis might have suggested that the $met^{2G/2G}$ mice were normal, and that the $met^{2P/2P}$ and $met^{2S/2S}$ animals were probably both loss-of-function, because of the lower overall activation of Ras and PI3K. $met^{2G/2G}$ mice were in fact viable, fertile, and apparently normal, while the $met^{2P/2P}$ and $met^{2S/2S}$ mutants were both lethal. However, Met^{2S}, but not Met^{2P}, was sufficient for placental development, allowing $met^{2S/2S}$ embryos to survive until birth. Proliferation of fetal myoblasts, a relatively late event in myogenesis previously shown to be Met dependent (Maina et al., 1996), was also selectively rescued by Met^{2S}. In placental trophoblasts and fetal myoblasts, the function of HGF seems to be essentially proliferative. This suggests that Src activation may be central to this Met-mediated response. Although our biochemical data suggests Src binding to the multifunctional docking site, indirect activation of Src cannot be excluded. Regardless, this is strong genetic evidence for a direct role of a Src family member downstream of an RTK in vivo.

Neither Met^{2P} nor Met^{2S} were sufficient for HGF-mediated hepatocyte survival in the developing liver. On the other hand, Met^{2P} and Met^{2S} both resulted in the partial rescue of myoblast migration, insufficient to fully colonize the diaphragm, but allowing the development of selected muscle groups in the limbs. Precursors of appendicular and diaphragm muscles depend on HGF/Met to delaminate from the somite and to migrate to their destination (reviewed in Birchmeier and Gherardi, 1998). In our *met* mutants, where the receptor can signal properly through Gab1, reduction of muscle mass was comparable to that observed in the Gab1 knockout. This suggests that for full myoblast migration, both Gab1-dependent and Gab1-independent Met-mediated signals are required. Thus, we interpret the partial rescue seen in $met^{2P/2P}$ and $met^{2S/2S}$ embryos as the result of the residual net Gab1-mediated Met signaling, rather than as the effect of direct recruitment of Src or PI3K.

HGF has a broad spectrum of activities and synergies with other neurotrophic factors on a variety of neuron populations (reviewed in Maina and Klein, 1999). In vivo, *hgf* null and $met^{d/d}$ mutant mice display deficiencies in nerve outgrowth and branching consistent with the in vitro activities. However, since motoneurons depend on trophic factors secreted by muscle, and HGF is required for muscle development, some aspects of these in vivo defects could arise as a consequence of the muscle defect. Comparison of the phenotypes of $met^{2P/2P}$ and $met^{2S/2S}$ mutants provides strong evidence for a direct role of Met in neurons. In these mutants, limb muscles develop equally, but nerves develop differently. While in $met^{2S/2S}$ mutants, limb nerve deficiencies are similar to the *hgf* null and $met^{d/d}$ mutants, signaling in $met^{2P/2P}$ embryos is sufficient to promote axon outgrowth and branching of specific motor nerves. This was further confirmed by the fact that in $met^{2P/2P}$ mutants. HGF cooperates with NGF in promoting axon outgrowth of sympathetic neurons in vitro. This last observation suggests

that Met and TrkA may cooperate by promoting an adequate level of PI3K downstream signaling.

In this work, we have described knockin *met* mutants with optimal PI3K and Src binding motifs. Both mutants resulted in severe loss of function but differed in their rescue of specific cell types. The partial rescue of myoblast migration was the only trait in common, and most likely resulted from the net contribution of residual Gab1-mediated Met signaling. The rescue of placenta and fetal myoblast proliferation versus axon growth by Src or PI3K binding sites, respectively, indicates that Met-mediated developmental events require the activation of specific pathways above a necessary threshold of Gab1-mediated signaling. Our results suggest that shared multiadaptors may provide the threshold of generic signaling output upon which every receptor, according to its individual profile, superimposes qualitatively different signals to achieve specific biological responses.

Experimental Procedures

Generation of *met* Mutant Mice

Gene targeting was done by knockin as in Maina et al. (1996). In the new targeting vector, the *neo* cassette was flanked by LoxP sites for Cre-mediated removal in vivo (Schwenk et al., 1995). The presence of the neo cassette was assessed by PCR using oligonucleotide 1 in the *neo* cassette and oligonucleotide 2 (see Figures 2A and 2C). Specificity-switch mutants were genotyped using oligonucleotides 4 (in three different versions, specific for the *met*^{2P}, *met*^{2S}, or *met*^{2G} mutations) and 5 to amplify a fragment in the C-terminal portion of the human *Met* cDNA. Mice were kept on a mixed C57Bl/6x129/sv background for the analysis of placenta, migrating myoblasts, and nerve development. Backcrossing mutant mice into the outbred strain CD1 allowed us to partially rescue placental development and to establish primary cell cultures from E15.5 *met*$^{d/d}$ and *met*$^{2P/2P}$ mutant embryos (F1 CD1).

Growth Factors, Fusion Proteins, and Antibodies

GST-fusion proteins have been previously described (Ponzetto et al., 1994). The growth factors used were HGF (R&D Systems), insulin (Sigma), EGF (Boehringer Mannheim), and NGF (gift from Genentech). The antibodies used were anti-HGF (R&D Systems), anti-human and anti-mouse Met (Santa Cruz), anti-phospho Akt and anti-phospho ERKs (BioLabs), anti-phospho Src (44-658Z, BioSource International), anti-tubulin, anti-neurofilament, and anti-laminin (Sigma), anti-BrdU and FITC-conjugated sheep anti-mouse (Boehringer Mannheim), anti-desmin (DAKO), and cy-3-conjugated goat anti-mouse (Jackson Immunoresearch Laboratories).

Hepatocyte Cultures

Livers dissected from E15.5 embryos were digested with collagenase. Debris was removed by filtration through a sterile nylon filter (Falcon) and cells were collected by centrifugation. Cell suspensions were plated on collagen-treated dishes in hepatocyte attachment media (HAM; Gibco BRL), supplemented with 2% fetal calf serum and 10 ng/ml of insulin. After 4 hr attachment, the medium was replaced with HAM supplemented with 2% fetal calf serum, 10 ng/ml insulin, and 50 ng/ml EGF. Cells were starved 16 hr before HGF stimulation.

Myoblast Cultures

For myoblast cultures, E14.5 back muscles were digested with dispase II and DNase I (Boehringer Mannheim) in PBS. Debris was removed as described above. Cells were plated for 4 hr on collagen-treated dishes in a DMEM medium containing 20% horse serum (HS) and 0.5% CEE (ICN). The medium was changed for 10 hr to 2% HS without additives, with 10 ng/ml of HGF or 0.5% CEE, followed by an overnight incubation with BrdU. Cells were then fixed and BrdU-positive myoblasts were identified by immunofluorescence using anti-desmin and anti-BrdU antibodies. For each condition, at least 200 myoblasts were counted in three separate experiments. In vivo myoblast proliferation was evaluated as previously described (Maina et al., 1996).

Pull-Down, Western Immunoblotting, and Ras and PI3K Assays

Procedures of cell lysis, pull-down experiments, and Western blotting have been previously described (Ponzetto et al., 1994). For phospho Akt and ERKs analysis, total extracts were separated on 15% Anderson gels and immunoblotted with specific antibodies. The PI 3′-kinase inhibitor LY294002 (Calbiochem) was added 1 hr before HGF stimulation at 50 μM. Ras and PI3K assays were performed as described (Egea et al., 2000).

Histological Analysis, Whole-Mount In Situ Hybridization, and Immunohistochemistry

Histological analysis, phalloidin staining procedures, apoptotic cell detection, whole-mount in situ hybridization, and immunohistochemistry were done as previously described (Maina et al., 1996, 1997). To compare liver sizes, liver masses were corrected for reduction in embryo weight. For the quantification of the muscle mass, 10 μm transversal sections of the proximal part of E15.5 forelimbs were counterstained with toluidine blue. One section of each limb, taken at the upper level of the ossification center of the humerus, was used for muscle quantification. The area of recognizable limb muscles was measured with NIH Image software.

Sympathetic Neuron Cultures

Culture and in vitro axon outgrowth assays were performed as described (Maina et al., 1998).

Acknowledgments

We thank F. Casagranda and F. Diella for technical help with ES cells, K. Vintersten of the Transgenic Service for the generation of chimeric mice, L. Minichiello for providing anti-Gab1 antibody, I. Gout for anti-p85 antibodies, A. Porras for advice on embryonic hepatocyte cultures, W. Birchmeier for GST-Gab1, G. Superti-Furga, A. Nebreda, and A. Palmer for valuable comments on the manuscript, and Bob Milne for revising it. This work was in part supported by European Union Network Grants (Biotechnology to R.K. and A.M.D., and Biomed to C.P.), and by grants from the Wellcome Trust (A.M.D.) and Telethon Italy (D.095 to C.P.). The continuing support of the Compagnia di San Paolo and of the Fondazione CRT to C .P.'s laboratory is gratefully acknowledged.

Received May 17, 2000; revised April 26, 2001.

References

Bardelli, A., Basile, M.L., Audero, E., Giordano, S., Wennstrom, S., Menard, S., Comoglio, P.M., and Ponzetto, C. (1999). Concomitant activation of pathways downstream of Grb2 and PI 3-kinase is required for MET-mediated metastasis. Oncogene *18*, 1139–1146.

Birchmeier, C., and Gherardi, E. (1998). Developmental roles of HGF/SF and its receptor, the c-Met tyrosine kinase. Trends Cell Biol. *8*, 404–410.

Caton, A., Hacker, A., Naeem, A., Livet, J., Maina, F., Bladt, F., Klein, R., Birchmeier, C., and Guthrie, S. (2000). The branchial arches and HGF are growth-promoting and chemoattractant for cranial motor axons. Development *127*, 1751–1766.

Egea, J., Espinet, C., Soler, R.M., Peiro, S., Rocamora, N., and Comella, J.X. (2000). Nerve growth factor activation of the extracellular signal-regulated kinase pathway is modulated by Ca(2+) and calmodulin. Mol. Cell. Biol. *20*, 1931–1946.

Fambrough, D., McClure, K., Kazlauskas, A., and Lander, E.S. (1999). Diverse signaling pathways activated by growth factor receptors induce broadly overlapping, rather than independent, sets of genes. Cell *97*, 727–741.

Fixman, E.D., Holgado-Madruga, M., Nguyen, L., Kamikura, D.M., Fournier, T.M., Wong, A.J., and Park, M. (1997). Efficient cellular transformation by the Met oncoprotein requires a functional Grb2

binding site and correlates with phosphorylation of the Grb2-associated proteins, Cbl and Gab1. J. Biol. Chem. *272*, 20167–20172.

Holgado-Madruga, M., Moscatello, D.K., Emlet, D.R., Dieterich, R., and Wong, A.J. (1997). Grb2-associated binder-1 mediates phosphatidylinositol 3-kinase activation and the promotion of cell survival by nerve growth factor. Proc. Natl. Acad. Sci. USA *94*, 12419–12424.

Itoh, M., Yoshida, Y., Nishida, K., Narimatsu, M., Hibi, M., and Hirano, T. (2000). Role of Gab1 in heart, placenta, and skin development and growth factor- and cytokine-induced extracellular signal-regulated kinase mitogen-activated protein kinase activation. Mol. Cell. Biol. *20*, 3695–3704.

Maina, F., Casagranda, F., Audero, E., Simeone, A., Comoglio, P., Klein, R., and Ponzetto, C. (1996). Uncoupling of Grb2 from the Met receptor in vivo reveals complex roles in muscle development. Cell *87*, 531–542.

Maina, F., Hilton, M.C., Ponzetto, C., Davies, A.M., and Klein, R. (1997). Met receptor signaling is required for sensory nerve development and HGF promotes axonal growth and survival of sensory neurons. Genes Dev. *11*, 3341–3350.

Maina, F., Hilton, M.C., Andres, R., Wyatt, S., Klein, R., and Davies, A.M. (1998). Multiple roles for hepatocyte growth factor in sympathetic neuron development. Neuron *20*, 835–846.

Maina, F., and Klein, R. (1999). Hepatocyte growth factor - a versatile signal for developing neurons. Nat. Neurosci. *2*, 213–217.

Pawson, T., and Nash, P. (2000). Protein-protein interactions define specificity in signal transduction. Genes Dev. *14*, 1027–1047.

Pawson, T., and Saxton, T.M. (1999). Signaling networks - do all roads lead to the same genes? Cell *97*, 675–678.

Ponzetto, C., Bardelli, A., Zhen, Z., Maina, F., dalla Zonca, P., Giordano, S., Graziani, A., Panayotou, G., and Comoglio, P.M. (1994). A multifunctional docking site mediates signaling and transformation by the hepatocyte growth factor/scatter factor receptor family. Cell *77*, 261–271.

Sachs, M., Brohmann, H., Zechner, D., Muller, T., Hulsken, J., Walther, I., Schaeper, U., Birchmeier, C., and Birchmeier, W. (2000). Essential role of Gab1 for signaling by the c-Met receptor in vivo. J. Cell Biol. *150*, 1375–1384.

Schaeper, U., Gehring, N.H., Fuchs, K.P., Sachs, M., Kempkes, B., and Birchmeier, W. (2000). Coupling of Gab1 to c-Met, Grb2, and Shp2 mediates biological responses. J. Cell Biol. *149*, 1419–1432.

Schlessinger, J. (2000). Cell signaling by receptor tyrosine kinases. Cell *103*, 211–225.

Schwenk, F., Baron, U., and Rajewsky, K. (1995). A cre-transgenic mouse strain for the ubiquitous deletion of loxP-flanked gene segments including deletion in germ cells. Nucleic Acids Res. *23*, 5080–5081.

Simon, M.A. (2000). Receptor Tyrosine Kinases: specific outcomes from general signals. Cell *103*, 13–15.

Songyang, Z., Shoelson, S.E., Chaudhuri, M., Gish, G., Pawson, T., Haser, W.G., King, F., Roberts, T., Ratnofsky, S., Lechleider, R.J., et al. (1993). SH2 domains recognize specific phophopeptide sequences. Cell *72*, 767–778.

Tremblay, P., Kessel, M., and Gruss, P. (1995). A transgenic neuroanatomical marker identifies cranial neural crest deficiencies associated with the Pax3 mutant Splotch. Dev. Biol. *171*, 317–329.